Int. J. Heat Mass Transfer. Vol. 9, pp. 171–188. Pergamon Press 1966. Printed in Great Britain

PREDICTION OF TWO-PHASE ANNULAR FLOW WITH LIQUID ENTRAINMENT

S. LEVY

General Electric Company, Atomic Power Equipment Department, San Jose, California

(*Received* 28 *September* 1964 *and in revised form* 12 *August* 1965)

Abstract—An analytical prediction of two-phase annular flow with liquid entrainment is presented. The solution is obtained by considering the momentum and mass-transfer components of the interfacial shear and showing that the momentum term is dominant within the liquid film, while the mass-transfer term is the important component within the gas core.

An expression is derived for the interfacial shear in terms of liquid film thickness, and this equation is used:

(a) To correlate the available CISE film thickness data in circular pipes with two-phase flow of water or alcohol and argon or nitrogen at various pressures.
(b) To predict liquid film thickness, liquid film flow rate, and liquid entrainment in the gas core. Typical results are presented for steam–water mixtures flowing in circular pipes at high pressure.
(c) To compare the predicted values of liquid film thickness and flow rate with reported measurements in upwards, downwards and horizontal flow.

NOMENCLATURE

a, radius of core [cm];
b, pipe radius [cm];
D, diameter [cm];
G, mass flow per unit cross-sectional area [g/cm^2 s];
g, gravitational constant [980 cm/s^2];
K, mixing length constant, nondimensional;
l_u, mixing length for velocity [cm];
$l_{\rho u}$, mixing length for momentum [cm];
n, exponent on pressure drop grouping, nondimensional;
p, pressure [dyne/cm^2];
R, function of density ratio;
t, liquid film thickness [cm];
U, mean velocity [cm/s];
u, local velocity in flow direction [cm/s];
$(\rho u)'$, fluctuating component of local momentum in flow direction [cm/s];
v', fluctuating component of local velocity perpendicular to flow direction [cm/s];
X, weight fraction of gas or vapor, nondimensional;
y, distance measured from wall [cm];
z, distance measured along the flow direction [cm];
ρ, local density [g/cm^3];
σ, surface tension [dyne/cm];
τ, shear stress [dyne/cm^2].

Subscripts

c, core;
f, film;
G, gas;
L, liquid;
W, wall.

Superscripts

$+$, nondimensionalized as indicated by equations (12) and (13).

INTRODUCTION

THE MOST common flow pattern in two-phase systems is the annular or liquid film flow pattern. Several analytical solutions of this type of flow pattern have been presented, but the solutions deal only with the simplified case of a liquid film and gas core with a smooth interface and no liquid entrainment [1–6]. No predictions have yet been offered for the more practical case of a wavy liquid–gas interface and substantial liquid entrainment. It is the purpose of this report to deal analytically with the latter, and more complex, flow geometry. Because the interface shear and flow structure are expected to be intimately related, the mechanisms prevailing

at the interface are first examined. The findings at the interface are next applied to predict the liquid film flow rate, liquid film thickness, and liquid entrainment under various flow conditions.

INTERFACE SHEAR

In a turbulent flow system where the fluid density is not constant, the local shear stress τ is equal to [7, 8]

$$\tau = -\overline{(\rho u)'v'} \tag{1}$$

In equation (1), ρ and u are the mean components of density and velocity in the flow direction, while $(\rho u)'$ and v' are the fluctuating components of momentum in the flow direction and of velocity in the direction perpendicular to it. Since the fluid density is not constant, the variation of density with position must be taken into account in the definition of the shear stress τ. It can indeed be shown that the variation of density is significant at a gas–liquid interface. Let us, for instance, consider two adjacent and parallel streams as shown in Fig. 1. One stream is made up of a thin film, containing mostly liquid, flowing along the channel wall. The second stream occupies the central portion of the channel and consists of gas laden with liquid particles. The velocity and density profiles in the two streams are shown schematically in Fig. 1, but for the sake of simplification, we shall use the mean streams fluid density and velocity; i.e. ρ_f, ρ_c, U_f and U_c.

Let us next express the local fluctuating components of velocity and momentum in terms of their corresponding mixing length l_u and $l_{\rho u}$, or

$$\sqrt{(\overline{v'^2})} \approx \sqrt{(\overline{u'^2})} = l_u \frac{\mathrm{d}u}{\mathrm{d}y};$$

$$\sqrt{(\overline{\rho u)'^2}} = l_{\rho u} \left| \left(\frac{\mathrm{d}\rho u}{\mathrm{d}y} \right) \right|. \tag{2}$$

The local shear τ becomes

$$\tau = \rho l_u l_{\rho u} \left(\frac{\mathrm{d}u}{\mathrm{d}y} \right)^2 + u l_u l_{\rho u} \frac{\mathrm{d}u}{\mathrm{d}y} \left| \left(\frac{\mathrm{d}\rho}{\mathrm{d}y} \right) \right|. \tag{3}$$

The shear stress τ is made up of two terms: a momentum component $\rho l_u l_{\rho u} (\mathrm{d}u/\mathrm{d}y)^2$, and a mass-transfer component

$$u l_u l_{\rho u} \frac{\mathrm{d}u}{\mathrm{d}y} \left| \left(\frac{\mathrm{d}\rho}{\mathrm{d}y} \right) \right|.$$

The existence of both terms has been recognized for a long time in single-phase compressible flow [7], but the mass-transfer component has always been neglected because of the low velocity (i.e. negligible compressibility), near the channel wall. This assumption is not valid in two-phase flow, and its fallacy was first noted in reference [8] in a treatment of density variations in a two-phase stream.

The velocity and density gradients on the core side of the interface can be approximated* by

$$\frac{\mathrm{d}u}{\mathrm{d}y} \approx \frac{U_c - U_f}{a/2} \approx \frac{U_c - U_f}{b/2};$$

$$-\frac{\mathrm{d}\rho}{\mathrm{d}y} \approx \frac{\rho_f - \rho_c}{a/2} \approx \frac{\rho_f - \rho_c}{b/2}, \tag{4}$$

where a is the half width of the stream of density ρ_c and b the half channel width.

The shear stress τ_c on the core side of the interface is

$$\tau_c \approx \rho_c l_u l_{\rho u} \left(\frac{U_c - U_f}{b/2} \right)^2 + l_u l_{\rho u} U_c \left(\frac{U_c - U_f}{b/2} \right) \left(\frac{\rho_f - \rho_c}{b/2} \right). \tag{5}$$

Equation (5) can be rewritten as follows:

$$\tau_c \approx l_u l_{\rho u} U_c \left(\frac{U_c - U_f}{b/2} \right) \left(\frac{\rho_f - \rho_c}{b/2} \right) \left[1 + \frac{\rho_c}{\rho_f - \rho_c} \frac{U_c - U_f}{U_c} \right].$$

In most practical systems, $\rho_c \ll \rho_f - \rho_c$, and since $(U_c - U_f)/U_c \leqq 1$, the first term in equation (5), or the momentum component of core shear stress τ_c, is negligible with respect to mass-transfer term.

Similarly, on the liquid side of the interface closest to the channel wall, one can write

$$\left.\begin{aligned} &\frac{\mathrm{d}u}{\mathrm{d}y} \approx \frac{2U_f}{b-a}: \quad -\frac{\mathrm{d}\rho}{\mathrm{d}y} \approx \frac{2(\rho_L - \rho_f)}{b-a} \\ &\tau_L = \rho_f l_u l_{\rho u} \left(\frac{2U_f}{b-a} \right)^2 \left[1 + \frac{\rho_L - \rho_f}{\rho_f} \right] \end{aligned}\right\} \tag{6}$$

* Since ratios of $(\mathrm{d}u/\mathrm{d}y)$ to $(\mathrm{d}\rho/\mathrm{d}y)$ are subsequently used to evaluate the relative importance of the mass-transfer and momentum components of shear, the straight-line approximations assumed in equation (4) do not detract from the answer as long as the velocity and density profiles are relatively similar.

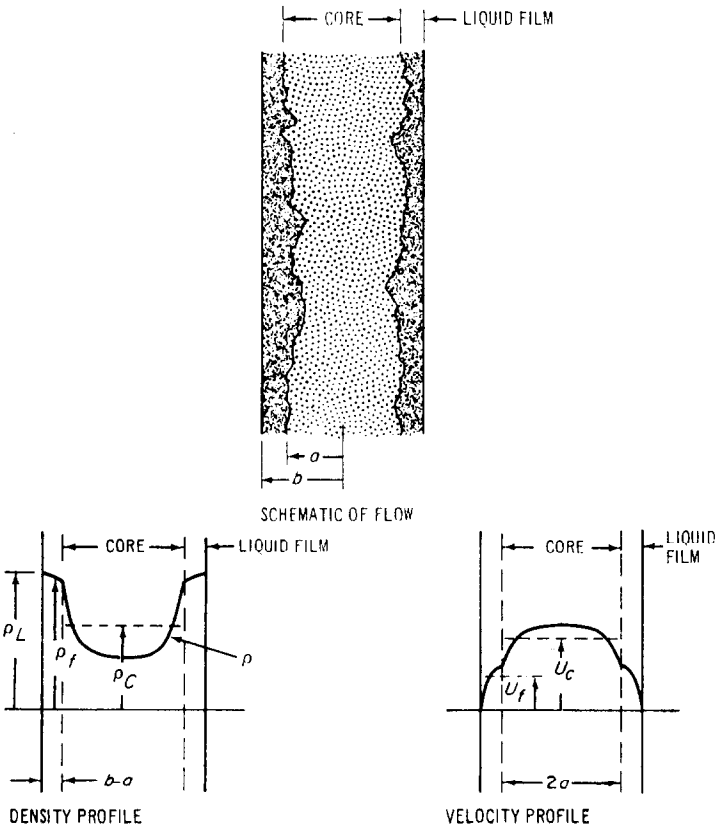

FIG. 1. Annular flow with liquid entrainment.

Here

$$\frac{\rho_L - \rho_f}{\rho_f} \ll 1,$$

and the mass-transfer component of shear stress is found to be negligible.

One could have inferred the same results by recognizing that, by definition, the liquid film has only a small, if not zero, density variation across it, and the variation of density across it equals zero; so does the mass-transfer component of shear stress. On the other hand, a very sharp density gradient exists within the core at the interface, and the shear mass-transfer term becomes the important component on the core side of the interface.

It is interesting to note that the above result has not been recognized in previous analytical treatment of a two-phase interface. Previous theoretical models, dealing with a pure liquid film and a pure gaseous core, postulated that

$$\left.\begin{aligned} \tau_f &= \tau_c \\ \tau_f &= \rho_L l_u^2 \frac{\mathrm{d}u_L^2}{\mathrm{d}y} \\ \tau_c &= \rho_G l_u^2 \frac{\mathrm{d}u_G^2}{\mathrm{d}y} \end{aligned}\right\} \quad (7)$$

where the subscripts L and G are used to represent the liquid and gas.

In equation (7), the liquid film is treated appropriately, which explains why the models give approximately correct results for the liquid film flow rate and for the two-phase pressure drop in terms of the liquid film flow rate [1, 5]. The solutions, however, do not recognize that there exists a sharp density gradient on the gas side of the interface and that the mass-transfer term is important there. This accounts for the

failure of the model to predict the slip ratio correctly (ratio of mean gas to liquid velocity). The solutions also fail grossly when compared to experimental data in their predictions of two-phase pressure drop in terms of gas flow rate in the core. It can be surmised that improved correlation with experimental results would be obtained by including the mass-transfer component of shear stress.

DERIVATION OF EQUATIONS

We shall consider here only the case of vertical upwards flow in a pipe, but the proposed solution, as pointed out later, can be readily extended to horizontal or downwards flow directions. If we neglect the mass-transfer term within the liquid film, and if we assume that the density within the film is constant and equal to ρ_L, we can write

$$\tau_f = \rho_L l_u \left(\frac{du_L}{dy}\right)^2. \tag{8}$$

Let us postulate next, as in single-phase flow, that

$$\tau_f = \tau_w, \qquad l_u = Ky \tag{9}$$

where τ_w is the wall shear stress and y is the distance measured from the wall.

If the gravitational forces are neglected with respect to shear forces, the velocity distribution in the turbulent section of the liquid film is given by

$$u_L = \frac{1}{K}\sqrt{\left(\frac{\tau_w}{\rho_L}\right)} \ln y + \text{constant}. \tag{10}$$

By taking K and the constant in equation (10) to be the same as in single-phase flow, there results

$$u_L^+ = \frac{u_L}{\sqrt{(\tau_w/\rho_L)}} = 2{\cdot}5 \ln \frac{y\sqrt{(\tau_w/\rho_L)}\,\rho_L}{\mu_L} + 5{\cdot}5 = 2{\cdot}5 \ln y^+ + 5{\cdot}5, \tag{11}$$

where μ_L is the liquid absolute viscosity and y^+ is, by definition,

$$y^+ = y\sqrt{\left(\frac{\tau_w}{\rho_L}\right)}\frac{\rho_L}{\mu_L}. \tag{12}$$

We can get similar expressions for the velocity in the laminar and buffer layer of the liquid film, or

$$\left.\begin{aligned} u_L^+ &= y^+ && y^+ < 5 \\ u_L^+ &= -3{\cdot}05 + 5{\cdot}00 \ln y^+ && 5 < y^+ < 30 \end{aligned}\right\} \tag{13}$$

The liquid film flow rate per unit area of pipe cross section, G_f, is obtained by integrating equations (11) and (13):

$$G_f = \frac{2}{b}\mu_L F(y^+), \tag{14}$$

where

$$\left.\begin{aligned} F(y^+) &= 3y^+ + 2{\cdot}5\, y^+ \ln y^+ - 64 && \text{for } y^+ > 30 \\ F(y^+) &= 12{\cdot}5 - 8{\cdot}05\, y^+ + 5y^+ \ln y^+ && 5 < y^+ < 30 \\ F(y^+) &= 0{\cdot}5y^{+2} && y^+ < 5 \end{aligned}\right\} \tag{15}$$

If G_G and G_L are used to represent the total gas and liquid flow rates per unit cross-sectional area of pipe, the gas weight fraction in the core, X_c, is equal to

$$X_c = \frac{G_G}{G_G + G_L - G_f}. \tag{16}$$

If the flow in the core is assumed to be homogeneous, the core average density ρ_c is equal to

$$\frac{1}{\rho_c} = \frac{1}{\rho_L}(1 - X_c) + \frac{1}{\rho_c} X_c. \tag{17}$$

The average film and core velocities U_c and U_f are then

$$\left.\begin{aligned} U_f &= \frac{G_f}{\rho_L}\frac{1}{1 - a^2/b^2} \\ U_c &= \frac{G_G}{X_c}\frac{b^2}{a^2}\frac{1}{\rho_c} \end{aligned}\right\} \tag{18}$$

Let us next examine the shear stress on the core side of the interface. By neglecting the momentum contribution to shear, we find from equation (5) with $\rho_L = \rho_f$ and $y^+ > 30$

$$\tau_c \approx l_u l_{\rho u} U_c \left(\frac{U_c - U_f}{b/2}\right)\left(\frac{\rho_L - \rho_c}{b/2}\right), \tag{19}$$

or

$$\sqrt{\left(\frac{l_u l_{\rho u}}{b}\right)} \approx 2\sqrt{\left(\frac{\tau_c}{U_c(\rho_L - \rho_c)(U_c - U_f)}\right)}. \tag{20}$$

In single-phase flow, the mixing length l has been found to be exclusively a function of the distance y measured from the channel wall. There is no reason to suspect a different behavior in two-phase flow and equation (20) can be written for $y^+ > 30$ as follows at the interface:

$$\sqrt{\left(\frac{\tau_c}{U_c(\rho_L - \rho_c)(U_c - U_f)}\right)} = F\left(\frac{b-a}{b}\right). \quad (21)$$

Equation (21) specifies the liquid film thickness $(b - a)$* in terms of the interface shear, the mean velocities U_L and U_c, and the densities ρ_L and ρ_c. When coupled with the preceding equations, equation (21) predicts the behavior of two-phase annular flow with liquid entrainment. The solutions can be expressed in terms of the total pressure drop per unit length $(-dp/dz)$ by realizing that

$$\left.\begin{aligned} \tau_w &= \left[\left(-\frac{dp}{dz}\right) - g\rho_L\left(1 - \frac{a^2}{b^2}\right) - g\rho_c\frac{a^2}{b^2}\right]\frac{b}{2} \\ \tau_c &= \left[\left(-\frac{dp}{dz}\right) - g\rho_c\right]\frac{a}{2} \end{aligned}\right\} \quad (22)$$

Equations (12), (14)–(18), (21) and (22) define the desired solution. Given the pressure $(-dp/dz)$ and the liquid film thickness $(b - a)$, we can solve the above equations for the function

$$F\left(\frac{b-a}{b}\right).$$

Once the universality of this function is established, we can use it to calculate the liquid film thickness, liquid film flow rate, and liquid entrainment for any given flow system where the pressure $(-dp/dz)$ can be calculated or measured. Before considering such solutions, it should be recognized that the above equations include two simplifications:

(1) The core flow was assumed to be homogeneous while in reality the gas is expected to slip with respect to the liquid particles contained in the core. The occurrence of slip has been noted by CISE [9]. Previous analyses [10, 11] have shown that the slip ratio or the ratio of mean gas to liquid velocity depends mostly upon the density fraction ρ_L/ρ_G. To approximately account for slip in this model, the left-hand side of equation (21) was multiplied by a function R of the density grouping (ρ_L/ρ_G). The function R is shown in Fig. 2 and can be approximated by $(\rho_L/\rho_G)^{1/3}$ for

$$1 < \rho_L/\rho_G < 200.$$

(2) In a previous report [6] it was shown that there exist two types of upwards annular flow with liquid entrainment. When the pressure drop $(-dp/dz)$ is greater than $g\rho_L$, the liquid film can dissipate more shear along the channel wall than it receives across the interface, and the interface waves are inferred to be small in amplitude. On the other hand, when $(-dp/dz)$ is smaller than $g\rho_L$, more shear is transmitted to the liquid than it can dissipate along the channel wall, and the interface waves are suspected to be large. Under the latter circumstances, the mixing length at the interface can be expected to be larger and this increase is assumed here to vary in proportion to the grouping

$$\left[\frac{g\rho_L}{(-dp/dz)}\right]^n.$$

The exponent n is subsequently shown to be equal to $\frac{1}{3}$. With these two semi-empirical corrections, we are now ready to consider the universality of the function

$$F\left(\frac{b-a}{b}\right).$$

CORRELATION OF AVAILABLE CISE FILM DATA IN TERMS OF DERIVED EQUATIONS

According to the previous section, one can write that

* The liquid film thickness is expected to vary with time and position in a two-phase steam. The symbol $(b - a)$ represents an equivalent mean film thickness averaged over time and position.

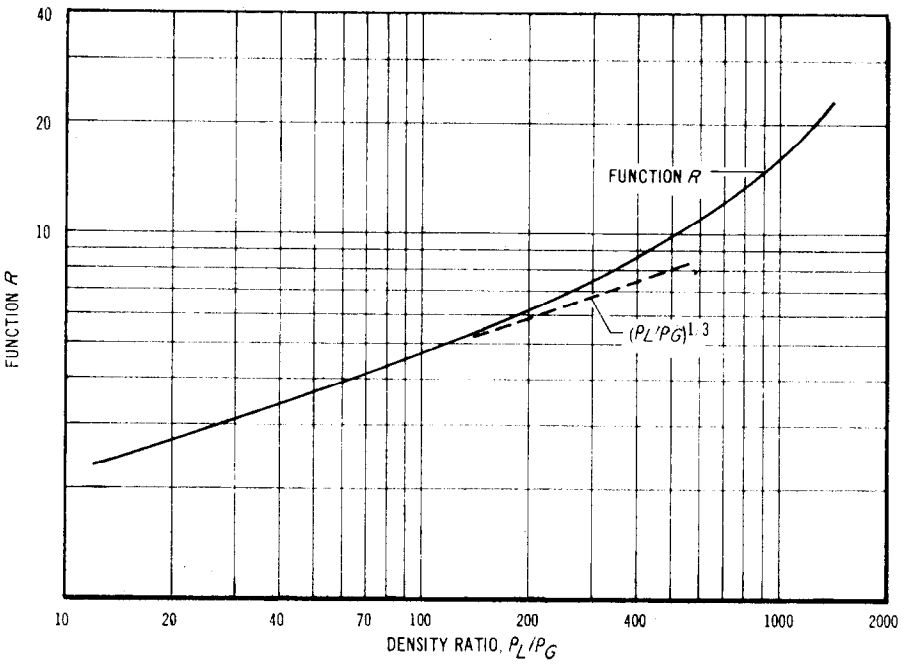

FIG. 2. Function R of the density ratio ρ_L/ρ_G.

$$\left.\begin{aligned}
&\sqrt{\left(\frac{\tau_c}{U_c(\rho_L-\rho_c)(U_c-U_f)}\right)}\,R(\rho_L/\rho_G)\\
&\qquad = F'\left(\frac{b-a}{b}\right) \text{ for } \left(-\frac{dp}{dz}\right) \geqq g\rho_L\\
&\sqrt{\left(\frac{\tau_c}{U_c(\rho_L-\rho_L)(U_c-U_f)}\right)}\,R(\rho_L/\rho_G)\\
&\qquad \left(\frac{g\rho_L}{-dp/dz}\right)^{-n} = F'\left(\frac{b-a}{b}\right)\\
&\qquad \text{for } \left(-\frac{dp}{dz}\right) < g\rho_L
\end{aligned}\right\} \quad (23)$$

Equations (23) can be combined with equations (12), (14)–(18) and (22) to determine the function

$$F'\left(\frac{b-a}{b}\right).$$

Data obtained at CISE in circular pipes [9, 12, 13] were used to calculate the function F'. The method of calculation uses the measured values of pressure drop $(-dp/dz)$ and liquid film thickness $(b-a)$, and solves for the function F'. The calculations were run through a computer and the results are shown in Figs. 3–6.

Figure 3 is a plot of the function F' for water–argon flow in a fixed tube size (2·5 cm), at a fixed set of density values (ρ_L = 1·0 g/cm^3 and ρ_G = 36·1 × 10^{-3} g/cm^3), and for $(-dp/dz)$ greater than $g\rho_L$. Figure 3 demonstrates the ability of equations (23) to bring together data taken at various argon and liquid flow rates. Very good correlation is obtained, and this correlation does not depend upon the correction factors

$$R\left(\frac{\rho_L}{\rho_G}\right) \quad \text{and} \quad \left[\frac{g\rho_L}{(-dp/dz)}\right]^{-n}$$

introduced into equations (23). The validity of these factors is, however, established in Figs. 4 and 5, where data obtained in the same tube are plotted for various argon densities and for $(-dp/dz) \leqq \rho_L g$. Good agreement with the mean curve of Fig. 3 is obtained for $n = \frac{1}{3}$ and for the function R shown in Fig. 2.

The ability of the factor F' to describe flow in a different pipe size or flow of a different fluid

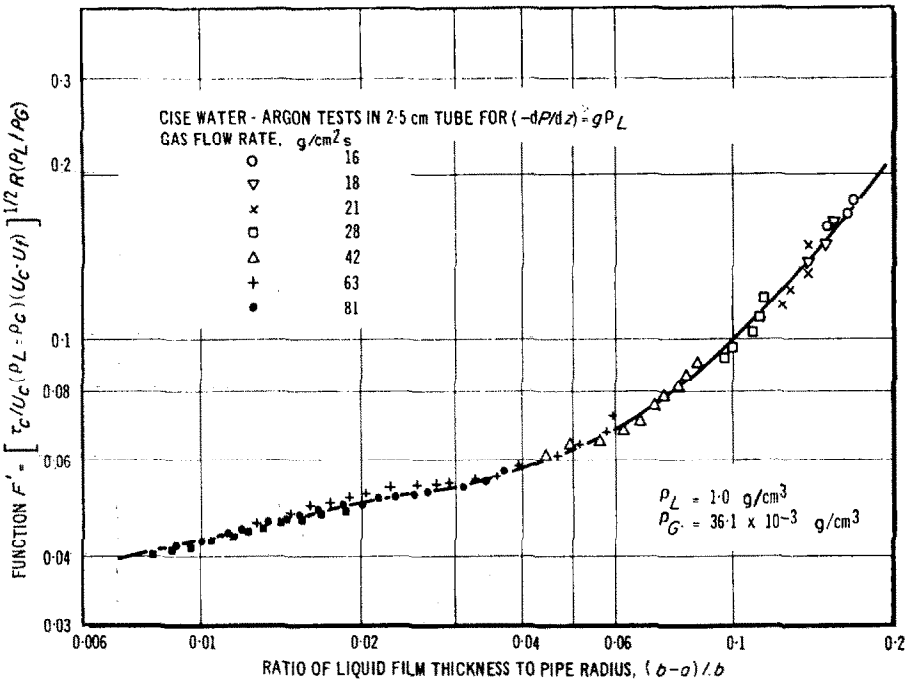

FIG. 3. Determination of function F' from CISE data for $(-\mathrm{d}p/\mathrm{d}z) \geqq g\rho_L$.

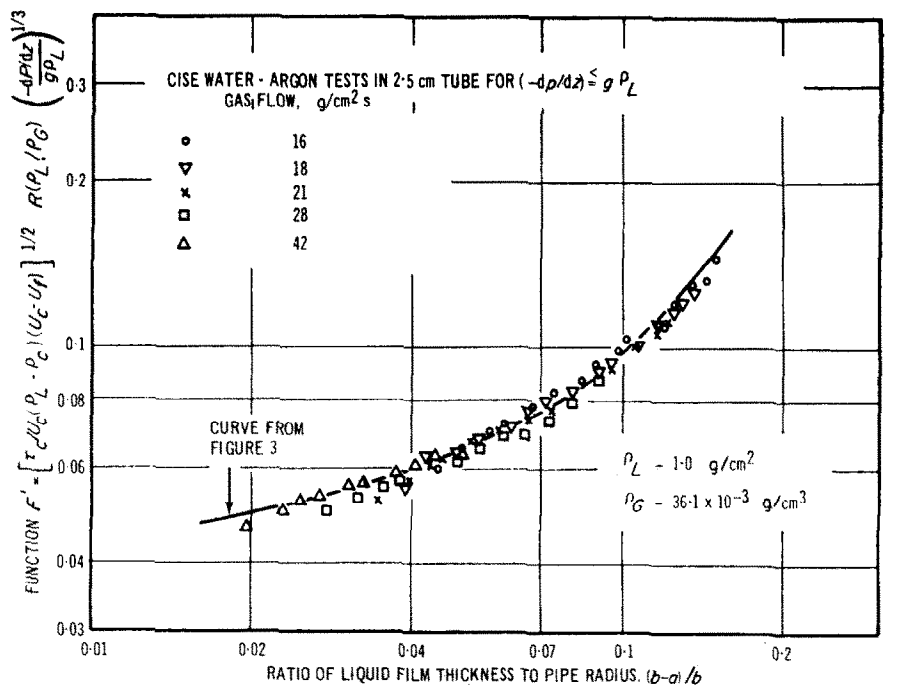

FIG. 4. Determination of function F' from CISE data for $(-\mathrm{d}p/\mathrm{d}z) \leqq g\rho_L$.

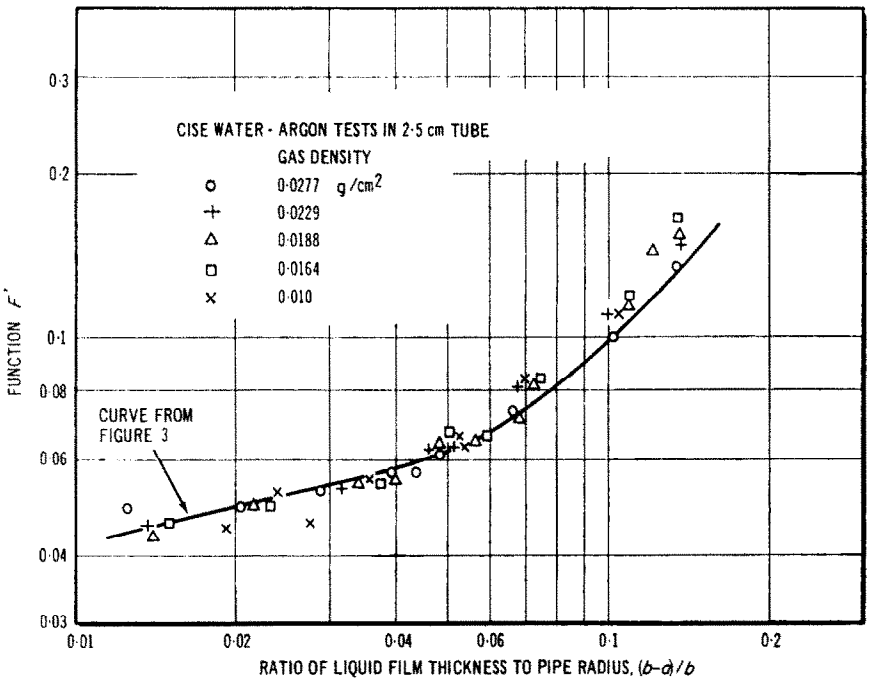

FIG. 5. Determination of function F' from CISE data at various gas densities.

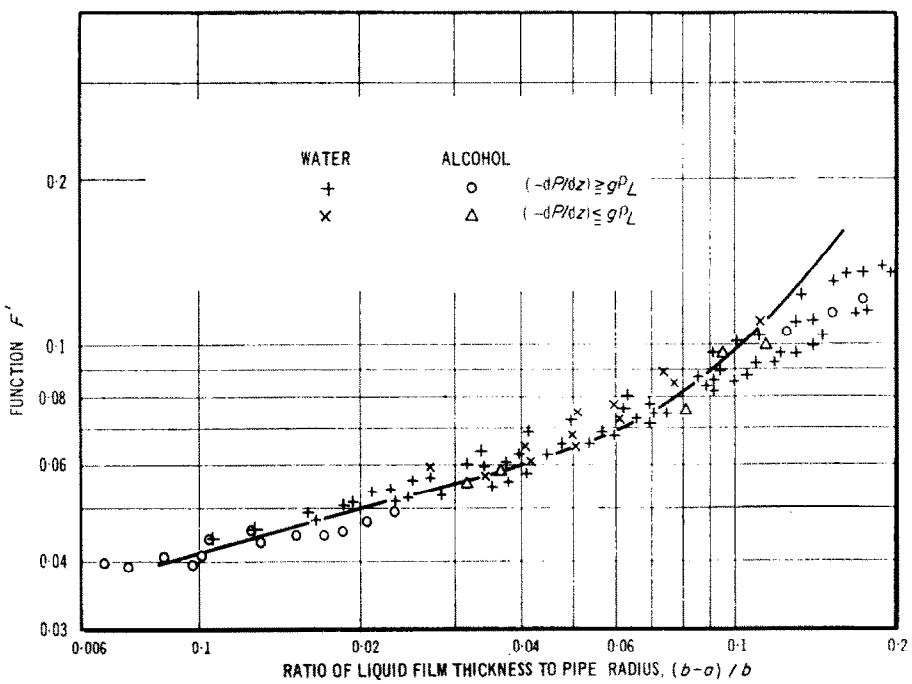

FIG. 6. Determination of function F' from CISE data with water and alcohol in 1·5 cm tube.

(alcohol) with a much lower surface tension is illustrated in Fig. 6 for pressure drops above and below $g\rho_L$. The spread in experimental data is slightly larger than in Figs. 3–5, but good agreement with the mean curve of Fig. 3 is again noted, except for large film thicknesses. When the film thickness exceeds 10 per cent of the pipe radius, the data for the 1·5 cm pipe tend to fall slightly below the curve of Fig. 3. The overall ability of equations (23) to correlate the CISE data is still very satisfactory when it is realized that measurements of two-phase pressure drop and liquid film thicknesses are expected to exhibit some inherent scatter.

Another method of evaluating the accuracy of equations (23) consists of applying the function F' as determined from Figs. 3–5 to calculate liquid film thicknesses. Before describing such computations, the basic equation will first be simplified to reduce the complexity of the calculations.

SIMPLIFIED EQUATIONS

Assume that the liquid film thickness is small so that $(a/b) = 1$. Postulate next that the gas density is much smaller than the liquid density

$$\left(\frac{\rho_G}{\rho_L} \ll 1\right).$$

It can then be shown that the following approximations are possible:

$$\frac{1}{\rho_c} = \frac{1}{\rho_G} X_c; \quad U_c = \frac{G_G}{\rho_G};$$

$$\rho_L \gg \rho_c; \quad \left(\frac{-\mathrm{d}p}{\mathrm{d}z}\right) \gg g\rho_c; \quad U_c \gg U_L. \quad (24)$$

The interface shear τ_c is equal to

$$\tau_c = \left(\frac{-\mathrm{d}p}{\mathrm{d}z}\right)\frac{b}{2}, \quad (25)$$

and equations (23) become

$$\sqrt{\left(\frac{(-\mathrm{d}p/\mathrm{d}z)(b/2)}{\rho_L}\right)}\frac{\rho_G}{G_G}R(\rho_L/\rho_G)\left(\frac{g\rho_L}{-\mathrm{d}p/\mathrm{d}z}\right)^{-n} = F'\left(\frac{b-a}{b}\right), \quad (26)$$

where $n = 0$ for $(-\mathrm{d}p/\mathrm{d}z) \geqq g\rho_L$ and $n = \frac{1}{4}$ for $(-\mathrm{d}p/\mathrm{d}z) \leq g\rho_L$.

Equation (26) is a considerable improvement over equations (23) because it directly gives the liquid film thickness in terms of the pressure drop $(-\mathrm{d}p/\mathrm{d}z)$. It no longer requires, as equations (23) do, reiterations of the liquid film flow rate to obtain the film thickness.

The validity of the simplified equation (26) is shown in Figs. 7–9. Figure 7 is a plot of a large portion of the CISE data obtained with water and alcohol in 2·5 and 1·5 cm tubes for an argon density of $36{\cdot}1 \times 10^{-3}$ g/cm^3 and $(-\mathrm{d}p/\mathrm{d}z) > g\rho_L$. Very good correlation of the data is obtained, and the mean line shown in Fig. 7 is only slightly different from the mean line plotted in Figs. 3–6. Ability to correlate data for $(-\mathrm{d}p/\mathrm{d}z) < g\rho_L$ and for lower gas densities is clearly illustrated in Figs. 8 and 9. In fact, it appears that the approximate equations are just as good as the more exact relations. This justifies their exclusive use in the following sections.

APPLICATION OF SIMPLIFIED EQUATIONS TO PREDICT ANNULAR FLOW WITH ENTRAINMENT IN CIRCULAR PIPES

For a given pipe size and for a specified set of liquid and gas flow rates and properties, the calculations proceed as follows. First the pressure drop $(-\mathrm{d}p/\mathrm{d}z)$ is computed by one of the many methods available in the literature [9, 14, 15]. The liquid film thickness is next obtained from equation (26) and the mean curve shown in Figs. 7–9. The liquid film flow rate is then calculated from equations (14) and (15), with the wall shear stress τ_w determined from the simplified equation

$$\tau_w = [(-\mathrm{d}p/\mathrm{d}z) - g\rho_L(1 - a^2/b^2)]\, b/2. \quad (27)$$

The liquid entrainment in the gas core is finally deduced by subtracting the liquid film flow rate from the total liquid flow.

This calculation method was first applied to two test runs reported by CISE [9]; the predicted liquid film thicknesses are shown in Fig. 10 together with the measured data. The total pressure drop $(-\mathrm{d}p/\mathrm{d}z)$ used in the calculations was obtained from the following correlation proposed by CISE [9, 12].

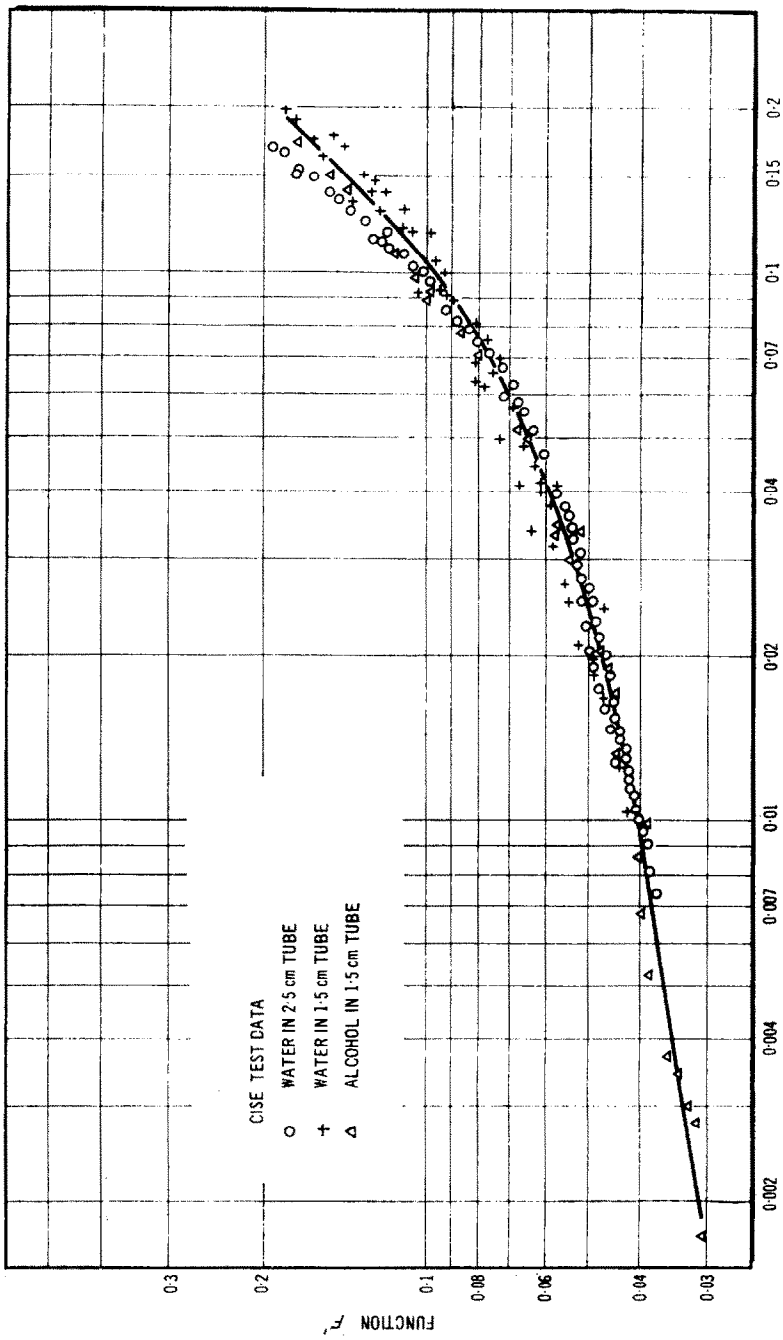

FIG. 7. Determination of function F' from approximate equations for $(-\mathrm{d}p/\mathrm{d}z) \geqq \rho g$.

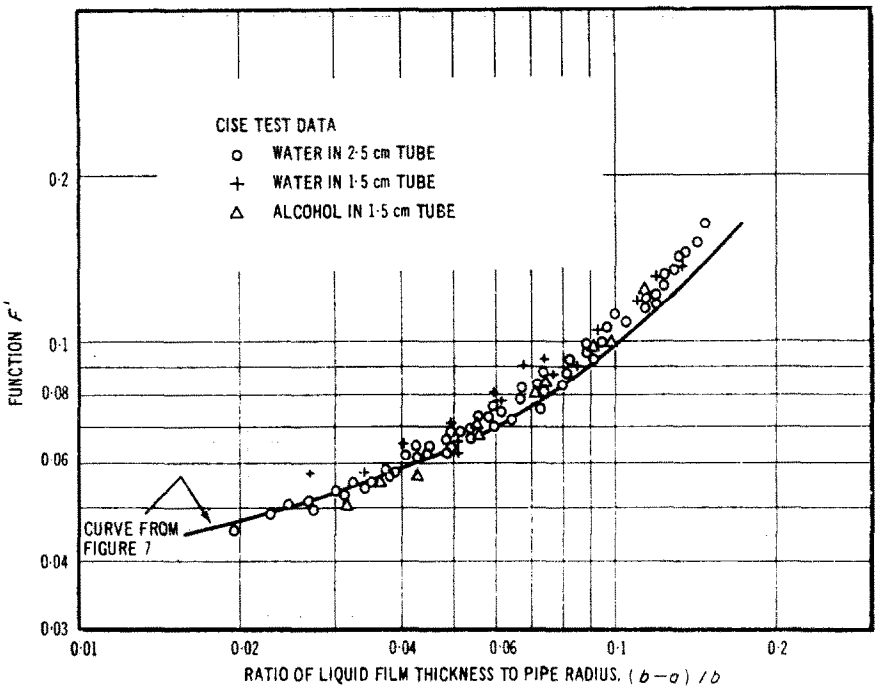

FIG. 8. Determination of function F' from approximate equations for $(-\mathrm{d}p/\mathrm{d}z) \leqq g\rho_L$.

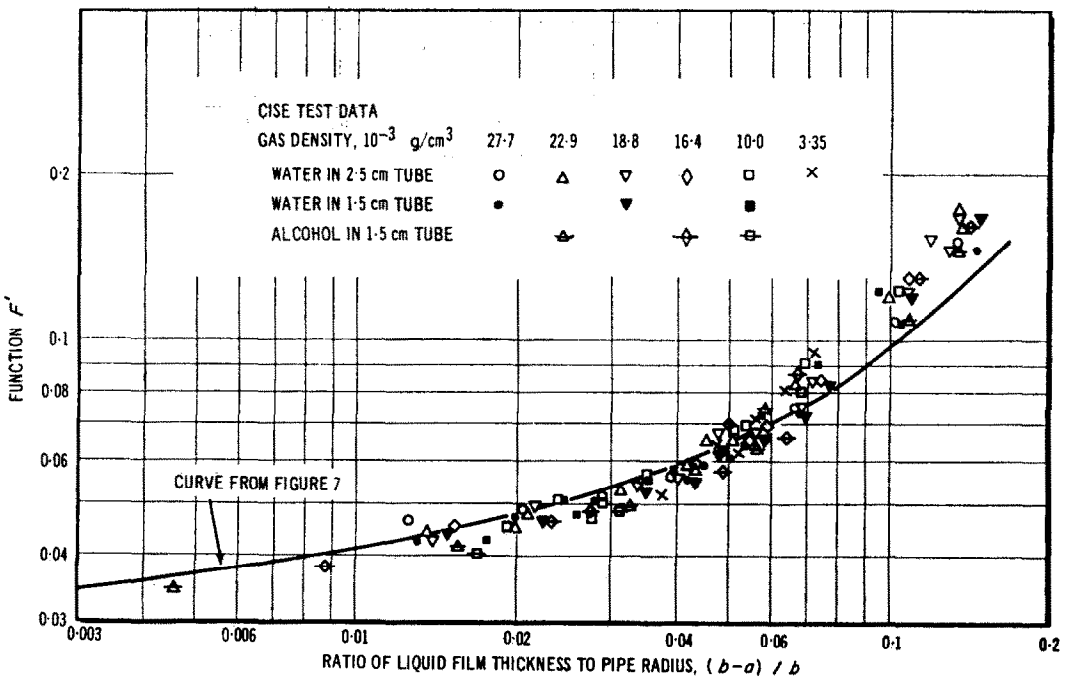

FIG. 9. Determination of function F' from approximate equations for various gas densities.

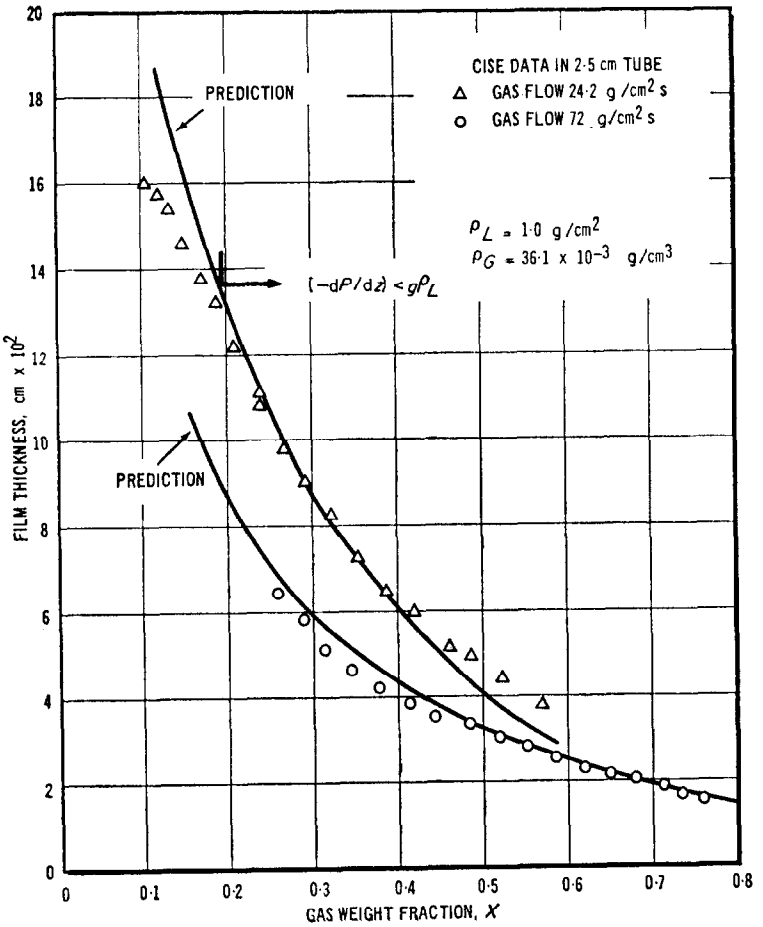

FIG. 10. Prediction liquid of film thickness in circular pipe.

$$\left(\frac{-dp}{dz}\right) = \left[g\Big/\left(\frac{G_L}{G_L+G_G}\frac{1}{\rho_L}+\frac{G_G}{G_L+G_G}\frac{1}{\rho_G}\right)\right] + \frac{0{\cdot}43}{(2b)^{1{\cdot}2}}\left(\frac{\sigma}{73}\right)^{0{\cdot}4}\left[(G_L+G_G)^2\left(\frac{G_L}{G_L+G_G}\frac{1}{\rho_L}+\frac{G_G}{G_L+G_G}\frac{1}{\rho_G}\right)\right]^{0{\cdot}75} \quad (28)$$

In equation (28), all units are in the cgs system, and σ is the surface tension.

The comparison between measurements and predictions is very good, as might be expected. Furthermore, the calculations and the experimental measurements show that for a constant gas flow rate the liquid film thickness decreases as the liquid flow decreases. Also, for the same gas weight fraction, the liquid film thickness is smaller at the higher gas flow rate. Furthermore, one finds that the liquid film thickness decreases as the surface tension or gas density is reduced. More generally, it can be observed that at a fixed gas flow rate, a large pressure gradient means a high liquid film thickness.

Another set of calculations was performed for upwards flow of steam–water mixtures at 70·3 kg/cm² (1000 psia) in a smooth 1·25 cm

(0·5 inch) pipe. Total flow rates of 68 and 136 g/s cm^2 (corresponding to 0·5 and 1·0 × 10^6 lb/h ft^2) were used in the calculations. The pressure drop ($-dp/dz$) was estimated from the Martinelli–Nelson [15] correlations. The results are shown in Fig. 11. It is seen that, according to the proposed model, the liquid film thickness decreases with increased steam quality and total flow rate. The percentage of liquid flowing in the film is also observed to decrease with increased steam quality and total flow rate. While the trends predicted by the analysis appear physically correct, there are, unfortunately, no experimental data which can confirm them. Particularly worthy of note is the fact that the present model predicts that more and more liquid is entrained from the film as the steam quality is increased. This lends credence to the recent arguments of Grace [16] that liquid entrainment from the film, rather than deposition, may be the controlling mechanism in two-phase annular flow with heat addition. Two other interesting comments can be made about the analytical model:

1. There exists today one other theoretical analysis of liquid film thickness in two-phase flow. Tippets [17] considered the stability of the interface and found that the film thickness was given by

$$(b - a)\tau_w \propto \frac{[(\rho_L/\rho_G) + 1]}{[1 + \sqrt{(\rho_L/\rho_G)}]^2}. \qquad (29)$$

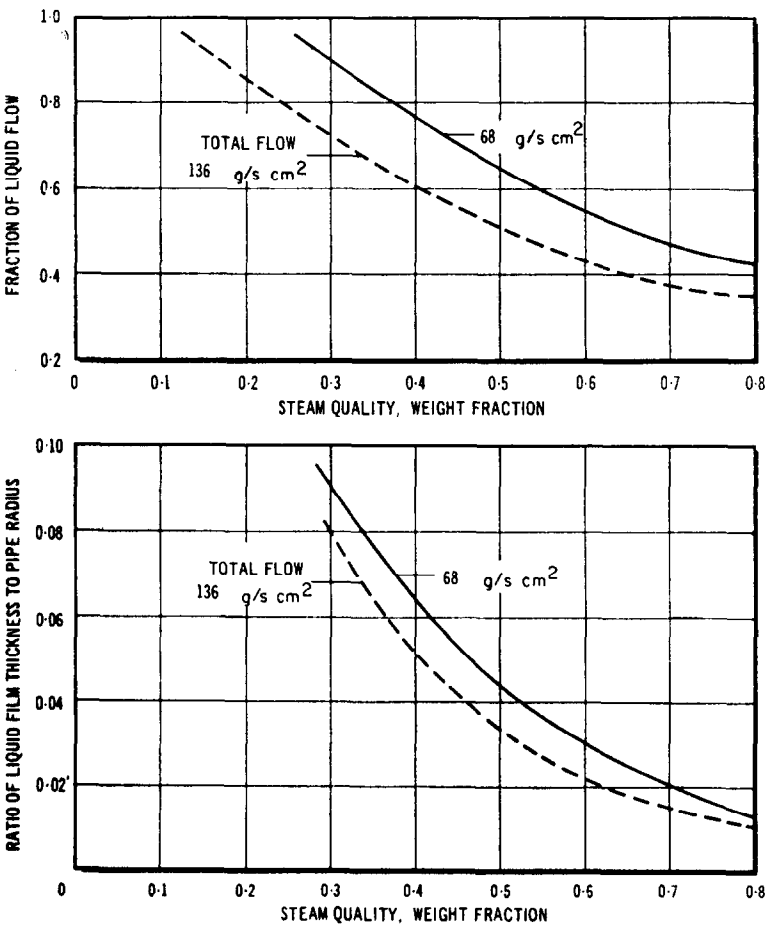

FIG. 11. Prediction of two-phase annular steam–water flow with liquid entrainment in a 1·25 cm tube at 70 kg/cm^2.

Equation (29) was applied to the CISE data, and the test results could not be correlated when the measured values of $(b - a)$ and τ_w were substituted in equation (29). Equation (29), in fact predicts the opposite trend from the measured one as the pressure drop increases. It is possible that the difficulty with equation (29) stems from the fact that Tippets neglected the mass-transfer component of shear and used equations (7) to describe the conditions at the interface.

2. The proposed model can be extended to more complex geometries. A tentative prediction of upwards two-phase annular flow with liquid entrainment in an annular geometry is, for instance, given in reference [18].

COMPARISON OF PROPOSED MODEL TO OTHER AVAILABLE TEST DATA

Before applying the proposed model to other available test data, it is important to reiterate two of its shortcomings. First, the model is only valid in the turbulent core, i.e. $y^+ > 30$. For $y^+ < 30$, additional effects than those treated come into play, and the suggested relationship between film thickness and pressure drop does not apply. One can surmise that in the laminar and buffer layers, liquid will not be entrained as easily; and the liquid film thickness will decrease much more slowly with pressure drop. Second, when the proposed model is used to predict a liquid film thickness, one must check that the predicted liquid film rate does not exceed the total available liquid flow; if it does, the liquid film flow rate should be taken equal to the total liquid flow and the corresponding film thickness backcalculated. Once these limitations are recognized, the model can be applied to reported experimental data of two-phase annular flow in the upwards, downwards, and horizontal directions.

Upwards vertical flow

Test results have been reported by Gill and Hewitt [19] for air–water mixtures near atmospheric pressure. By utilizing the reported

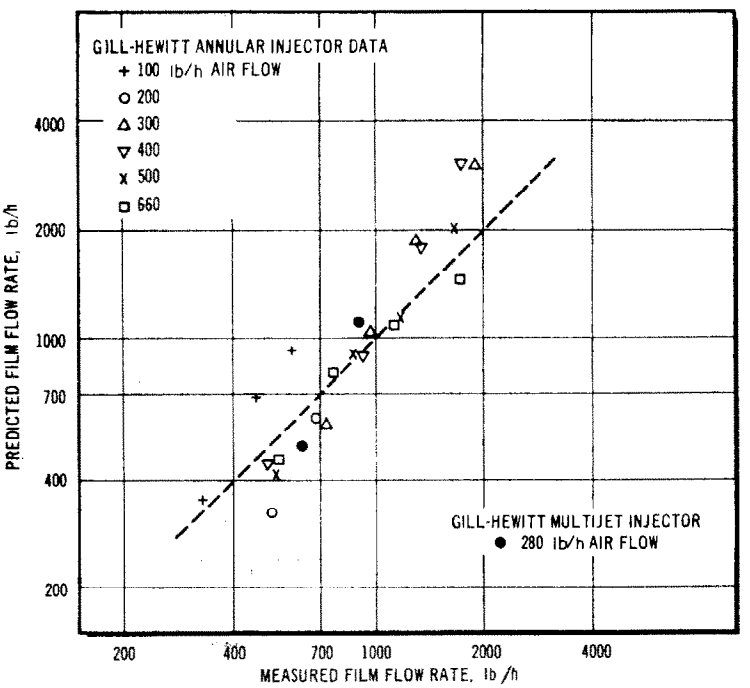

FIG. 12. Comparison of proposed model with test data in upwards vertical flow.

nonaccelerational pressure drop, it is possible to calculate the liquid film thickness and the liquid film flow rate for values of y^+ in excess of 30. The results obtained for the liquid film flow rate with an annular slot injector with the simplified equation (26) are compared to the measured values in Fig. 12. It is observed that the predictions compare satisfactorily with the test data at high gas flow rates. At the lower gas flow rates and especially at high liquid rates, the model tends to overpredict the film flow rates. This comes about because the simplified equations neglect hydrostatic losses and thus overestimate the liquid film thickness. At the lower gas flow rates, the pressure drop is small. The head losses become more and more important, and the use of the more exact equations is recommended to obtain better agreement. Examination of Fig. 12 also shows that the model tends to underpredict the film flow rates at low liquid rates. These points correspond to values of y^+ very close to 30. As previously noted, if the present model were to be applied at y^+ less than 30, it would predict much lower film thicknesses than measured. A similar trend has been noted when comparing CISE and Harwell film thicknesses [19]. The Harwell film thicknesses at reduced liquid flow rates were found to be much larger than would be predicted by the empirical correlation of CISE results. It was felt originally that such a deviation was due to the different methods employed in measuring the liquid film thickness. This possibility has since been disproved [20]. A more plausible explanation of the difference between CISE and Harwell data follows the line proposed above. Practically all the CISE film thicknesses fall in the region of $y^+ > 30$. At reduced liquid flow rates, the Harwell film thicknesses can be shown to give values of $y^+ < 30$. In the laminar and buffer layers, the liquid film thickness decreases much more slowly and the Harwell data should fall well above the CISE correlation which is based upon film thicknesses in the turbulent core.

A similar degree of agreement was obtained between predictions and measurements for the Gill–Hewitt results with a multijet injector, as shown for a typical case in Fig. 12. As the entrance conditions are changed, the pressure drop varies and equation (26) still applies.

Downward vertical flow

Mean liquid film thicknesses in downwards vertical flow have been reported by Chien and Ibele [21] for air–water mixtures near atmospheric pressure. Application of equation (26) with $n = 0$ together with the measured values of interfacial shear stress gives the predictions shown in Fig. 13 for superficial gas velocities of 300, 150, 100 and 50 ft/s. Good agreement is obtained at the higher gas velocities. At 50 ft/s, the agreement is not as good. Here again, the head losses cannot be neglected; and if the more exact equations and the measured values of static pressure gradient had been used, the comparison between tests and predictions would be improved. A straight line corresponding to $y^+ = 30$ has been drawn in Fig. 13. It clearly shows the tendency of the measured film thicknesses to level off at $y^+ < 30$, while equation (26) continues to show a rapid decrease in liquid film thickness.

Horizontal flow

By setting n equal to zero and neglecting all other gravitational effects, equation (26) becomes applicable to horizontal flow. Some caution is, however, necessary before utilizing it. McManus [22] has measured liquid film thicknesses in horizontal flow and found a substantial variation of the liquid film size around the circumference. The proposed model does not allow for asymmetry in the flow distribution and should only be applied to those cases where the circumferential variations are small, i.e. small tube diameters and high pressure gradients. A typical comparison of the model with the data obtained by Wicks and Dukler [23] in a 1 inch tube is shown in Fig. 14 for $y^+ > 30$. The measured entrained flows were used to calculate the film thickness and the reported pressure drops to determine the function F'. The experimental points of F' versus liquid film thickness were then plotted in Fig. 14 together with the suggested curve of Figs. 8 and 9. The agreement is acceptable, with the test results tending to be slightly high. Good agreement was also obtained with the mean film thickness values of McManus in a 1 inch pipe at high pressure drops; but the comparison was poor

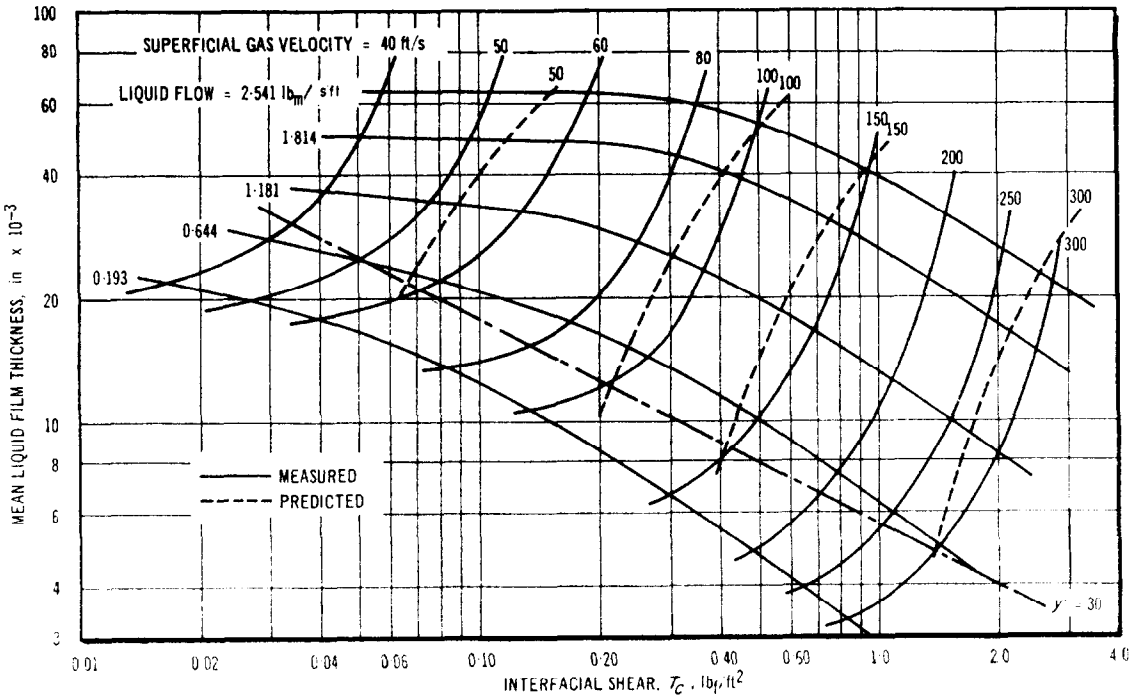

FIG. 13. Comparison of proposed model with test data in downwards vertical flow.

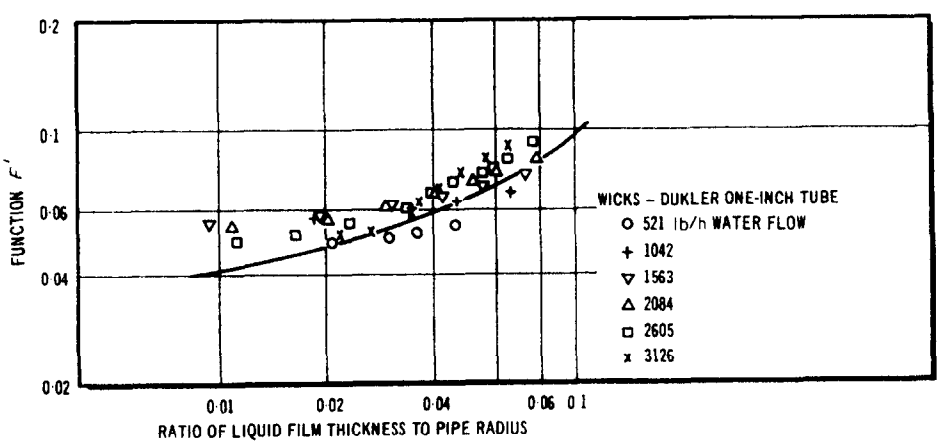

FIG. 14. Comparison of model with test data in horizontal flow.

for the 2 inch pipe where the pressure drop was low and considerable asymmetry existed.

Examination of Figs. 11–13 shows that the proposed simplified model gives an approximate, yet acceptable, prediction of two-phase annular flow. The comparison must, however, be limited to the conditions where the model is applicable, i.e. $y^+ > 30$, symmetrical flow conditions, and not excessively high head losses.

CONCLUSIONS

(1) An analytical description is offered for two-phase annular flow with liquid entrainment. The model compares satisfactorily with most of the available experimental data.

(2) Additional analysis and experimental data are needed to further check and improve the analytical model.

ACKNOWLEDGEMENTS

The author wishes to acknowledge the help of R. T. Bellan who computerized the solutions presented in Figs. 3–6. The work was performed under the U.S. Atomic Energy Commission Contract No. *AT*(04-3)-189, Project Agreement 27. Their support is acknowledged gratefully.

REFERENCES

1. S. Levy, Theory of pressure drop and heat transfer for annular steady-state two-phase, two-component flow in pipes, *Proceedings of the 2nd Midwestern Conference on Fluid Mechanics* (1952).
2. S. Calvert and B. Williams, Upwards co-current annular flow of air and water in smooth tubes, *A.I.Ch.E. Jl* **1**, 78 (1955).
3. G. H. Anderson and B. G. Mantzouranis, Two phase (gas–liquid) flow phenomena—I. Pressure drop and hold-up for two-phase flow in vertical tubes, *Chem. Engng Sci.* **12**, 109 (1960).
4. A. E. Dukler, Fluid mechanics and heat transfer in vertical falling film system, A.I.Ch.E. Preprint 101 (1959).
5. G. F. Hewitt, Analysis of annular two-phase flow: Applications of the Dukler analysis to vertical upward flow in a tube, AERE-*R*-3680 (1961).
6. S. Levy, Annular flow without liquid entrainment, *GEAP*-4195 (1963).
7. C. C. Lin, *Turbulent Flows and Heat Transfer*, p. 107. Princeton University Press (1959).
8. S. Levy, Prediction of two-phase pressure drop and density distribution from mixing length theory, *J. Heat Transfer* **85**, 137 (1963).
9. N. Adorni, I. Casagrande, L. Cravarolo, A. Hassid and M. Silvestri, Experimental data on two-phase adiabatic flow: Liquid film thickness, phase and velocity distribution, pressure drops in vertical gas–liquid flow, CISE, Report *R*35 (1961).
10. S. Levy, Steam slip-theoretical prediction from momentum model, *J. Heat Transfer* **82**, 113 (1960).
11. S. M. Zivi, Estimation of steady-state steam void fraction by means of the principle of minimum enthropy production, ASME Paper No. 63-*HT*-16 (1963).
12. N. Adorni, I. Casagrande, L. Cravarolo, A. Hassid, E. Pedrocchi and M. Silvestri, Further investigations in adiabatic dispersed two-phase flow: Pressure drop and film thickness measurements with different channel geometries—Analysis of the influence of geometrical and physical parameters. CISE Report *R*-53, (1963).
13. I. Casagrande, L. Cravarolo, A. Hassid and E. Pedrocchi, Adiabatic dispersed two-phase flow: Further results on the influence of physical properties on pressure drop and film thickness, CISE Report *R*-73, (1963).
14. R. W. Lockhart and R. C. Martinelli, Proposed correlation of data for isothermal two-phase, two-component flow in pipes, *Chem. Engng Prog.* **45** (1944).
15. R. C. Martinelli and D. B. Nelson, Prediction of pressure drop during forced circulation boiling of water, *Trans. Am. Soc. Mech. Engrs* **70**, 695 (1948).
16. J. M. Grace, The mechanism of burnout in initially subcooled forced convective systems, Ph.D. Thesis, University of Minnesota (1963).
17. F. E. Tippets, Analysis of the critical heat flux condition in high pressure boiling water flows, *J. Heat Transfer*, **86**, 23 (1964).
18. S. Levy, Prediction of two-phase annular flow with liquid entrainment, *GEAP*-4615 (May 1964).
19. L. E. Gill and G. F. Hewitt, Further data on the upwards annular flow of air–water mixtures, AERE *R*-3935 (1962).
20. G. F. Hewitt and P. C. Lovegrove, Comparative film thickness and holdup measurements in vertical annular flow, AERE *M*-1203 (1963).
21. S. F. Chien and W. Ibele, Pressure drop and liquid film thickness of two-phase annular and annular-mist flows, ASME Paper No. 62-*WA*-170 (1962).
22. H. N. McManus Jr., Local liquid distribution and pressure drops in annular two-phase flow, ASME Paper No. 61-*HYD*-20 (1961).
23. M. Wicks and A. E. Dukler, Entrainment and pressure drop in concurrent gas–liquid flow. Part I—Air-water mixtures in horizontal flow, *A.I.Ch.Jl* **6**, 463 (1960).

Résumé—On présente ici une théorie mathématique de l'écoulement annulaire diphasique avec entrainement de liquide. La solution est obtenue en considérant les composantes du cisaillement interfacial dû à la quantité de mouvement et du transport de masse et en montrant que le terme de

quantité de mouvement est prédominant à l'intérieur du film liquide, tandis que le terme de transport de masse est le plus important à l'intérieur du noyau gazeux.

Une expression est obtenue pour le cisaillement interfacial en fonction de l'épaisseur du film liquide, et l'on emploie cette équation:

(a) Pour corréler les données de la CISE sur l'épaisseur du film dans des tuyaux circulaires avec un écoulement diphasique d'eau ou d'alcool et d'argon ou d'azote à différentes pressions.

(b) Pour prédire l'épaisseur et le débit du film de liquide, et l'entraînement de liquide dans le noyau gazeux. Des résultats typiques sont présentés pour des mélanges d'eau et de vapeur s'écoulant dans des tuyaux circulaires à pression élevée.

(c) Pour comparer les valeurs prévues de l'épaisseur du film et du débir avec les mesures publiées pour les écoulements ascendants, descendants et horizontaux.

Zusammenfassung—Eine analytische Behandlung einer Zweiphasenströmung mit einem von Flüssigkeitströpfchen erfüllten Gasraum wird gegeben. Die Lösung ehrält man durch eine Untersuchung der Impuls- und Stofftransportkomponenten des Trennflächenschubs indem man zeigt, dass der Impulstransport im Flüssigkeitsfilm bestimmend ist, wahrend der Stofftransport die wichtige Komponente für den Gasraum darstellt. Unter Benützung der Flüssigkeitsfilmdicke ist ein Ausdruck für den Trennflächenschub abgeleitet; er wird verwendet um:

(a) die verfügbaren Daten der CISE Filmdicke in Rohren mit Kreisquerschnitt und Zweiphasenströmung von Wasser oder Alkohol mit Argon oder Stickstoff bei verschiedenen Drücken zu korrelieren,

(b) die Filmdicke der Flüssigkeit, ihre Strömungsgeschwindigkeit und die Flüssigkeitsladung des Gasraumes zu bestimmen. Typische Ergebnisse werden für Dampf-Wassergemische angegeben, die unter hohem Druck in Rohren mit Kreisquerschnitt strömen,

(c) die ermittelten Werte der Filmdicke der Flüssigkeit und die Geschwindigkeit mit angegebenen Messwerten für Aufwärts-, Abwärts- und Horizontalströmung zu vergleichen.

Аннотация—Проведен аналитический расчет двухфазного течения в кольцевом режиме при наличии уноса жидкости. Решение получено путем рассмотрения компонентов переноса кодичества движения и массы в напряжении трения на поверхности раздела. При этом показано, что влияние переноса количества движения преобладает в жидкой пленке, тогда как массоперенос играет существенную роль в газовом ядре.

Получено уравнение для напряжения трения на поверхности раздела, выраженного через толщину жидкой иленки. Это уравнение применяется:

(а) для обобщения известных данных по толщине пленки при течении в круглых трубах двухфазного потока воды или спирта и аргона или азота при различных давлениях;

(б) для расчета толщины жидкой пленки, скорости течения жидкой пленки и уноса жидкости в газовом ядре. Приведены типичные данные для течения пароводяных смесей в круглых трубах при высоком давлении;

(в) для сравнения расчетных значений толщины жидкой пленки и скорости течения с опубликованными данными измерений в восходящих и горизонтальных потоках.